Zeitschrift: IABSE publications = Mémoires AIPC = IVBH Abhandlungen
Band: 32 (1972)

Artikel: Discrete analysis of cylindrical orthotropic curved bridge decks
Autor: Buragohain, D.N.
DOI: https://doi.org/10.5169/seals-24939

Discrete Analysis of Cylindrical Orthotropic Curved Bridge Decks

Analyse discontinue de chaussées de ponts courbes cylindriques et orthotropes

Unstetige Analyse zylindrischer orthotroper gebogener Brückenfahrbahnen

D. N. BURAGOHAIN
Ph. D., Assistant Professor in Civil Engineering, Indian Institute of Technology, Bombay, India

Introduction

The increasing use of curved bridges in modern highways and highway interchanges has created considerable interest in the analysis of such structures. A curved bridge may either be a box-section bridge or may consist of a deck slab with curved longitudinal girders with or without radial cross-girders. In the latter case, the structure may be treated as an equivalent cylindrical orthotropic curved slab in which the longitudinal girders may be treated as flexible supports for the slab or their stiffness properties may be merged with the slab. COULL and DAS [1] have presented exact analytical solutions for isotropic curved slabs with simply-supported straight edges. Orthotropic curved plate theory has been presented by YONEZAWA [2] and others and used by HEINS and HAILS [3] for analysis of stiffined curved plates using finite difference and by BELL and HEINS [4] for simply-supported curved bridge decks on flexible curved girders using a slope-deflection formulation. CHEUNG [5], on the other hand, has presented a finite strip solution for simply supported curved bridge decks possessing orthotropic properties. This paper reports the development of a discrete energy formulation for orthotropic curved slabs with arbitrary boundary conditions.

The development of the discrete energy formulation for straight isotropic slabs has already been reported [6]. The same technique has also been extended to isotropic curved slabs using polar coordinates [7]. The present formulation incorporates cylindrical orthotropic properties of the curved slab to make it directly applicable to the analysis of curved bridge decks.

Comparison of results of two illustrative examples are presented. The first

example is of an isotropic curved slab with simply supported straight edges analysed by COULL and DAS [1] and CHEUNG [5]. The second one is of a stiffened curved plate analysed by HEINS and HAILS [3]. Experimental results are available for both these examples.

Method of Analysis

The scheme of structural discretisation and the coordinate system (r, Φ, z) are shown in Fig. 1, and the arrangement of nodes for the two classes of ele-

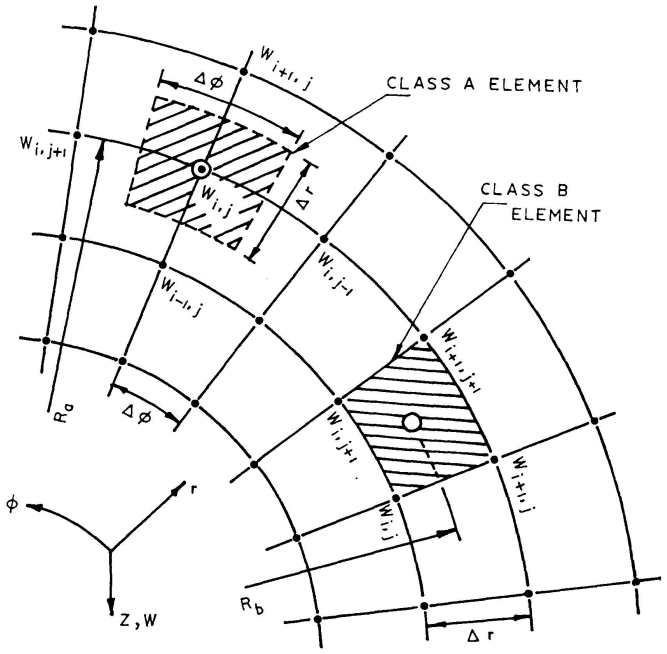

Fig. 1. Element discretization.

ments, class A and class B, are shown in the same figure. The total potential energy of the system is discretised into energy due to bending, contributed by class A elements, and energy due to twisting, contributed by class B elements. The potential energy π_a and π_b for class A and class B elements respectively will now be expressed in terms of the element nodal displacements using orthotropic theory.

Class A elements: The nodal displacements associated with class A elements are shown in Fig. 1 and the displacement vector $\{\delta_a\}$ is written as:

$$\{\delta_a\} = \{w_{i,j}\, w_{i+1,j}\, w_{i-1,j}\, w_{i,j+1}\, w_{i,j-1}\}^T, \tag{1}$$

where the right hand side denotes a column matrix written as the transpose of a row matrix. Using the classical thin plate theory, the internal strain components for a curved plate in bending consists of the curvatures χ_r and χ_Φ in r and Φ directions respectively, given by:

$$\{\epsilon_a\} = \begin{Bmatrix} \chi_r \\ \chi_\Phi \end{Bmatrix} = \begin{Bmatrix} -\dfrac{\partial^2 w}{\partial r^2} \\ -\left(\dfrac{\partial w}{r\,\partial r} + \dfrac{\partial^2 w}{r^2\,\partial \Phi^2}\right) \end{Bmatrix}. \tag{2}$$

If an equally spaced grid is used for discretisation with Δr and $\Delta \Phi$ as the intervals in the r and Φ directions respectively, the right hand side of Eq. (2) may be expressed in finite difference form and the strain components $\{\epsilon_a\}$ will be related to the displacements $\{\delta_a\}$ through the relation matrix $[B_a]$ as:

$$\{\epsilon_a\} = \begin{Bmatrix} -\dfrac{w_{i+1,j} - 2w_{i,j} + w_{i-1,j}}{\Delta r^2} \\ -\left(\dfrac{w_{i+1,j} - w_{i-1,j}}{2R_a \Delta r} + \dfrac{w_{i,j+1} - 2w_{i,j} + w_{i,j-1}}{R_a^2 \Delta \Phi^2}\right) \end{Bmatrix} = [B_a]\{\delta_a\}, \tag{3}$$

where
$$[B_a] = \begin{bmatrix} \dfrac{2}{\Delta r^2} & \dfrac{-1}{\Delta r^2} & \dfrac{-1}{\Delta r^2} & 0 & 0 \\ \dfrac{2}{R_a^2 \Delta \Phi^2} & \dfrac{-1}{2R_a \Delta r} & \dfrac{1}{2R_a \Delta r} & \dfrac{-1}{R_a^2 \Delta \Phi^2} & \dfrac{-1}{R_a^2 \Delta \Phi^2} \end{bmatrix}. \tag{4}$$

The stress resultants for class A elements consist of the bending moments M_r and M_Φ in the radial and tangential directions respectively. Using cylindrical orthotropic theory, the stress resultants $\{N_a\}$ can be expressed in terms of the strain components $\{\epsilon_a\}$ through the elasticity relations as

$$\{N_a\} = \begin{Bmatrix} M_r \\ M_\Phi \end{Bmatrix} = [D_a]\{\epsilon_a\}, \tag{5}$$

where
$$[D_a] = \begin{bmatrix} D_r & D_1 \\ D_1 & D_\Phi \end{bmatrix}. \tag{6}$$

In Eq. (6), the radial and tangential bending rigidities D_r and D_Φ and the cross rigidity D_1 may be expressed more exactly as:

$$\begin{aligned} D_r &= \frac{E_r t^3}{12(1 - \nu_r \nu_\Phi)}, \qquad D_\Phi = \frac{E_\Phi t^3}{12(1 - \nu_r \nu_\Phi)}, \\ D_1 &= \frac{\nu_r E_\Phi t^3}{12(1 - \nu_r \nu_\Phi)} = \frac{\nu_\Phi E_r t^3}{12(1 - \nu_r \nu_\Phi)}, \end{aligned} \tag{7}$$

in which E_r, ν_r and E_Φ, ν_Φ are the modulus of elasticity and Poisson's ratio in the radial and tangential directions respectively. For an isotropic material

$$E_r = E_\Phi = E \quad \text{and} \quad \nu_r = \nu_\Phi = \nu. \tag{8}$$

The potential energy of a class A element is then obtained as

$$\pi_a = \iint \tfrac{1}{2}\{\delta_a\}^T [B_a]^T [D_a][B_a]\{\delta_a\} r\, dr\, d\Phi - \{\delta_a\}^T \{q\}, \tag{9}$$

where $\{q\}$ represents the external surface forces on the element, given by

$$\{q\} = \{Q \ 0 \ 0 \ 0 \ 0\}^T \tag{10}$$

in which $Q = P$ for a concentrated load P at node $w_{i,j}$
and $Q = \int\int p_z r\, dr\, d\Phi$ for uniformly distributed load p_z normal to the slab.

Since all the matrices of Eq. (9) are constant, Eq. (9) may be written as:

$$\pi_a = \tfrac{1}{2}\{\delta_a\}^T [B_a]^T [D_a][B_a]\{\delta_a\} \Delta S_a - \{\delta_a\}^T \{q\}, \tag{11}$$

where ΔS_a is the class A elemental area given by $\Delta S_a = R_a \Delta r \Delta \Phi$, and $Q = p_z R_a \Delta r \Delta \Phi$ for uniformly distributed load.

Minimising the potential energy, the equilibrium equations are obtained from the condition $\delta \pi_a = 0$ as:

$$[B_a]^T [D_a][B_a]\{\delta_a\} \Delta S_a - \{q\} = 0, \tag{12}$$

which yields the class A element matrix $[k_a]$ as:

$$[k_a] = [B_a]^T [D_a][B_a] \Delta S_a \tag{13}$$

and $\{q\}$ as the element load vector.

Class B elements: The nodal displacements associated with the element for considering potential energy due to twisting alone are (Fig. 1):

$$\{\delta_b\} = \{w_{i+1,j+1}\, w_{i,j}\, w_{i+1,j}\, w_{i,j+1}\}^T. \tag{14}$$

The internal strains are due to the twisting curvature $\chi_{r\Phi}$ expressed by the strain matrix $\{\epsilon_b\}$ as:

$$\{\epsilon_b\} = \{\chi_{r\Phi}\} = \left\{-2\left(\frac{\partial^2 w}{r\,\partial r\,\partial \Phi} - \frac{\partial w}{r^2\,\partial \Phi}\right)\right\}. \tag{15}$$

Use of finite-difference relations in Eq. (15) to express $\{\epsilon_b\}$ in terms of $\{\delta_b\}$ through the relation matrix $[B_b]$ yields:

$$\begin{aligned}\{\epsilon_b\} &= \left\{-2\left(\frac{\partial^2 w}{r\,\partial r\,\partial \Phi} - \frac{\partial w}{r^2\,\partial \Phi}\right)\right\} \\ &= \left\{-2\left(\frac{w_{i+1,j+1} - w_{i+1,j} + w_{i,j} - w_{i,j+1}}{R_b \Delta r \Delta \Phi} - \frac{w_{i+1,j+1} + w_{i,j+1}}{2 R_b^2 \Delta \Phi} + \frac{w_{i,j} + w_{i+1,j}}{2 R_b^2 \Delta \Phi}\right)\right\} \\ &= [B_b]\{\delta_b\},\end{aligned} \tag{16}$$

where R_b = radius at the centre of class B element, and

$$[B_b]_{1\times 4} = [(c-d)\,(-c-d)\,(d-c)\,(c+d)], \tag{17}$$

where $$c = \frac{1}{R_b^2 \Delta \Phi} \quad \text{and} \quad d = \frac{2}{R_b \Delta r \Delta \Phi}.$$

The internal forces $\{N_b\}$ consist of the twisting moment $M_{r\Phi}$ alone and expressed in terms of the strain $\{\epsilon_b\}$ as:

$$\{N_b\} = \{M_{r\Phi}\} = \underset{1\times 1}{[D_b]}\{\epsilon_b\}, \tag{18}$$

where

$$\underset{1\times 1}{[D_b]} = [D_{r\Phi}]. \tag{19}$$

In Eq. (19), $D_{r\Phi}$ is the twisting rigidity given by $D_{r\Phi} = \frac{G_{r\Phi}\, t^3}{12}$, where $G_{r\Phi}$ is the shear modulus of elasticity. For an isotropic plate, $D_{r\Phi} = \frac{E\, t^3}{24\,(1+\nu)}$.

Following the same procedure as before, the potential energy of a class B element is obtained as

$$\begin{aligned} \pi_b &= \iint \tfrac{1}{2}\{\delta_b\}^T [B_b]^T [D_b][B_b]\{\delta_b\} r\, dr\, d\Phi \\ &= \tfrac{1}{2}\{\delta_b\}^T [B_b]^T [D_b][B_b]\{\delta_b\} \Delta S_b, \end{aligned} \tag{20}$$

where ΔS_b is the class B elemental area $R_b \Delta r \Delta \Phi$. No external load terms appear in Eq. (20), since all external loads are taken into account in class A elements.

On using the condition $\delta \pi_b = 0$, Eq. (20) yields the equilibrium equations as:

$$[B_b]^T (D_b][B_b]\{\delta_b\} \Delta S_b = 0 \tag{21}$$

and the class B element matrix $[k_b]$ as:

$$\underset{4\times 4}{[k_b]} = \underset{4\times 1}{[B_b]^T}\ \underset{1\times 1}{[D_b]}\ \underset{1\times 4}{[B_b]} \Delta S_b. \tag{22}$$

Boundary elements: Depending on its position along the boundaries, the class A element has eight other forms, denoted by A_2 through A_9 as shown in

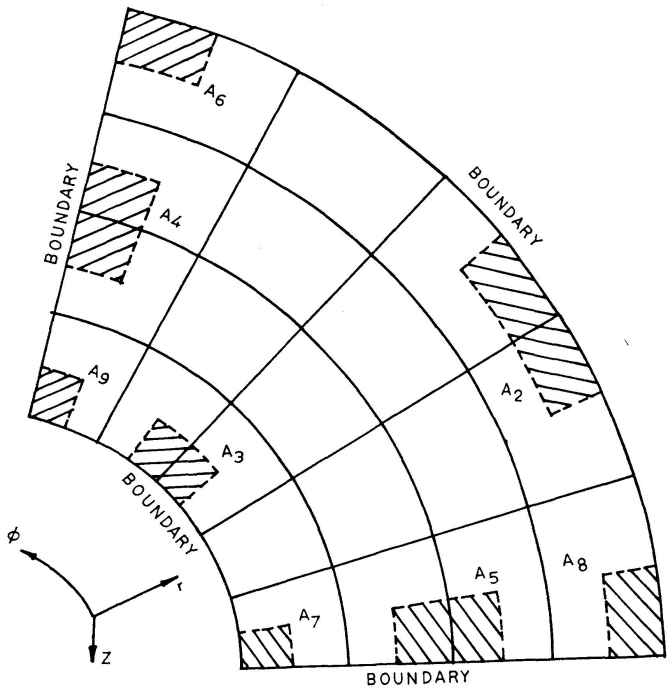

Fig. 2. Boundary elements.

Fig. 2, when the pivotal node $w_{i,j}$ lies on the boundary. For expressing $\{\epsilon_a\}$ in terms of displacements within the region, the rotation $\theta_1\left(=\frac{\partial w}{\partial r}\right)$ is introduced at the boundary r = constant, and the rotation $\theta_2\left(=\frac{\partial w}{r\,\partial \Phi}\right)$ is introduced at the boundary Φ = constant. Table 1 gives the finite difference expressions of the various terms in $\{\epsilon_a\}$ required for the boundary elements A_2 through A_9. The relation matrix $[B_a]$, the nodal displacement vector $\{\delta_a\}$ and the elemental area ΔS_a are modified accordingly for calculating the boundary element matrices according to Eq. (13).

Table 1. Finite difference expressions for different terms of strain components modified for boundary elements (see Fig. 2)

Terms of strain components	Finite difference expression for boundary elements	
	elements A_2, A_6, A_8[1])	elements A_3, A_7, A_9[1])
$\frac{\partial^2 w}{\partial r^2}$	$\frac{2(\Delta r\,\theta_{1\,i,j}+w_{i-1,j}-w_{i,j})}{\Delta r^2}$	$\frac{2(w_{i+1,j}-w_{i,j}-\Delta r\,\theta_{1\,i,j})}{\Delta r^2}$
$\frac{\partial w}{r\,\partial r}$	$\frac{\theta_{1\,i,j}}{R_a}$	$\frac{\theta_{1\,i,j}}{R_a}$
	elements A_4, A_6, A_9[1])	elements A_5, A_7, A_8[1])
$\frac{\partial^2 w}{r^2\,\partial \Phi^2}$	$\frac{2(R_a\Delta\Phi\,\theta_{2\,i,j}+w_{i,j-1}-w_{i,j})}{R_a^2\Delta\Phi^2}$	$\frac{2(w_{i,j+1}-w_{i,j}-R_a\Delta\Phi\,\theta_{2\,i,j})}{R_a^2\Delta\Phi^2}$

[1]) For elements not mentioned against a term, the expression for the term is the same as used in equation (3).

Overall stiffness matrix: The overall stiffness matrix $[k_T]$ and the overall load vector $\{q_T\}$ of the structure are obtained by taking the sum of all the element matrices and element load vectors respectively, arranged corresponding to the overall nodal displacement vector $\{\delta_T\}$:

$$[k_T] = \sum_i [k_i] \tag{23}$$

and

$$\{q_T\} = \sum_j \{q_j\}, \tag{24}$$

where i stands for all the elements A, A_2 through A_9 and B, and j stands for the elements A and A_2 through A_9. The equilibrium equation is then obtained as:

$$[k_T]\{\delta_T\} = \{q_T\}. \tag{25}$$

The unknown displacements $\{\delta_T\}$ are evaluated by solving Eq. (25).

Stress resultants: Knowing $\{\delta_T\}$, the element nodal displacement vector $\{\delta_a\}$ or $\{\delta_b\}$ may be formed for each element. The bending moments M_r and

M_Φ are evaluated at the pivotal node i,j of class A elements using Eqs. (3) and (5), and the twisting moment $M_{r\Phi}$ is evaluated at the centre of class B elements using Eqs. (16) and (18).

Illustrative Examples

Two numerical examples are analysed using the method outlined above. The first one is an isotropic curved plate simply-supported at the straight edges and the second is a stiffened curved plate exhibiting orthotropic properties. The details are given below:

Example 1: This example has been investigated experimentally and analytically by COULL and DAS [1] and also analytically by CHEUNG [5]. The structure consists of a 3/16 inch thick curved plate of black perspex of inner radius 7 inch and outer radius 13 inch and simply supported along the straight edges with an included angle of 60° between the supports (Fig. 3). Results are

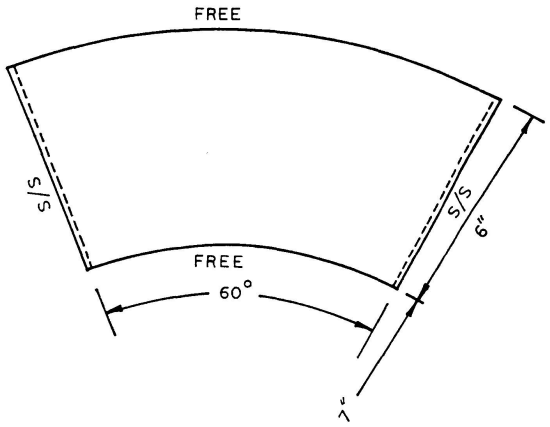

Fig. 3. Example 1.

obtained for three different load cases consisting of a unit concentrated load at mid-span at outer radius, mid-radius and inner radius. An 8×8 mesh is used in the present analysis.

Example 2: This example has been investigated experimentally and analytically by HEINS and HAILS [3]. It consists of a curved steel deck plate stiffened by 6 longitudinal curved girders of steel bulb Tee section (Fig. 4). The inner radius is 33.5 inch and outer radius 48.5 inch with the girders at equal intervals of 5 inch. The included angle is 120°. The supports are placed along the radial lines L_6 and R_6 and loads of 50 lb each are placed at the girders along the radial line R_3. This corresponds to the Run II test of HEINS and HAILS [3]. The orthotropic properties, determined by the authors [3] from model tests and adopted for analysis by finite difference, are

$D_r = 0.477 \times 10^3$ lb-in., $D_\Phi = 2631 \times 10^3$ lb-in.

and $D_{r\Phi} = 13.8 \times 10^3$ lb-in. with $\nu_r = \nu_\Phi = 0$.

The same values are used in the present analysis.

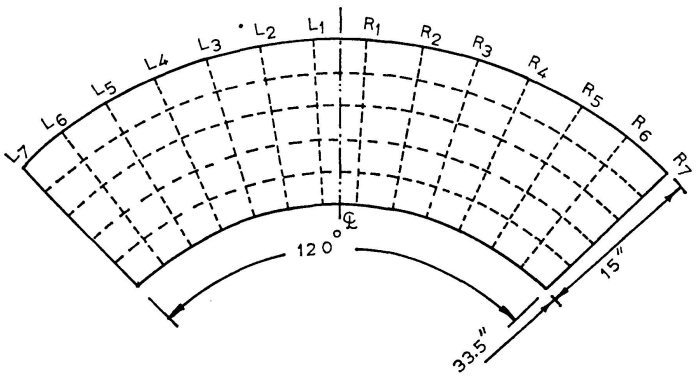

Fig. 4. Example 2.

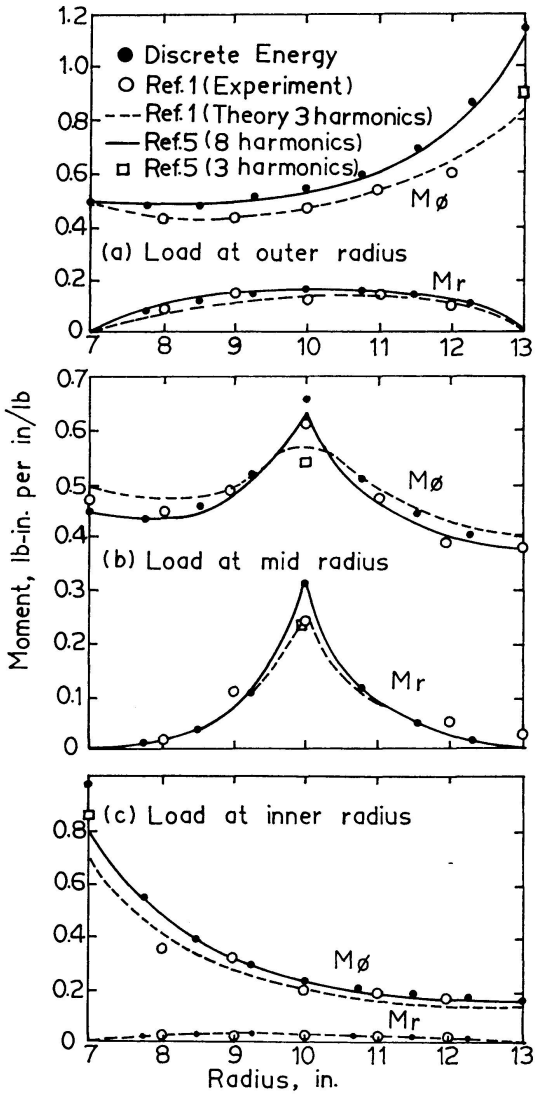

Fig. 5. Comparison of moments. Example 1.

Comparison of results: For example 1, the comparison of radial moments M_r and tangential moments M_Φ at mid-span is shown in Fig. 5. Poisson's ratio is taken as $\nu = 0.35$. Theoretical and experimental values of COULL and DAS [1] and the theoretical values of CHEUNG [5] are taken for comparison. It is seen that the results obtained by the "discrete energy" method proposed here are closer to those obtained by Cheung's finite strip method using 8 harmonics. At the points of application of loads, values of moments given by "discrete energy" method are higher than those of the finite strip method. It may be inferred that with the use of a greater number of harmonics the finite strip values will approach the "discrete energy" values. Eight curved finite strips have been used in Cheung's analysis while the present analysis uses an 8×8 mesh. Values of moments obtained by using 3 harmonics as reported in references 1 and 5 are generally lower. The difference is greater in the neighbourhood of concentrated loads and this may be attributed to the slow convergence of moments in the vicinity of concentrated loads.

For example 2, the radial distribution of deflection along the radial line L_1 (Fig. 4) and the circumferential distribution of deflection along the outer girder are compared with the experimental and theoretical values of HEINS and HAILS [3] and are shown in Fig. 6. It is seen that the results obtained by the "discrete energy" method using both the 5×11 mesh (5 panels radially and 11 panels circumferentially) and the 10×11 mesh are nearer to the experimental values. Furthermore, the difference between the results of these

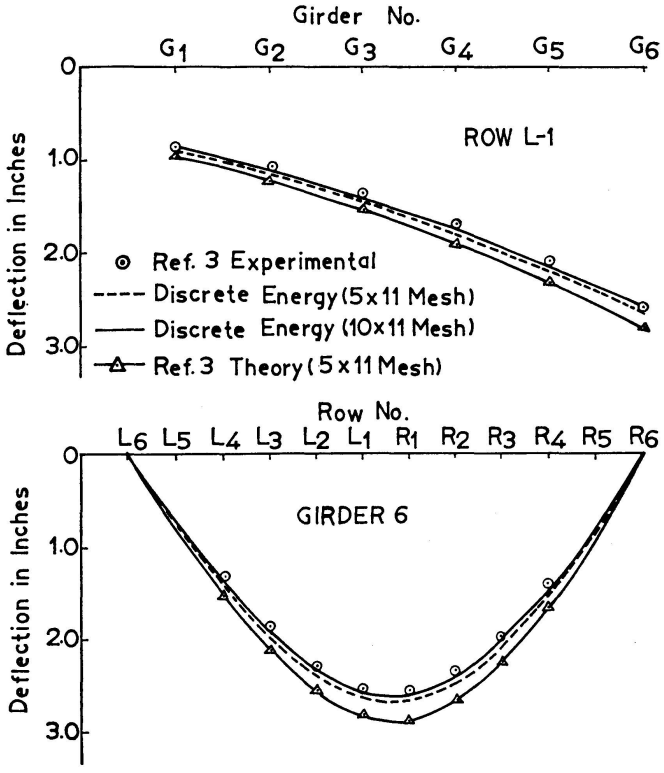

Fig. 6. Comparison of deflections. Example 2.

two meshes is very less. This emphasises the fact that even a coarse mesh can yield vera satisfactory results of deflections for the discrete energy method.

A Fortran program prepared for this formulation has taken approximately one minute on the CDC 3600 Computer to obtain each set of results. Half-banded Gaussian elimination technique has been used for the solution of the matrix equation.

Conclusions

It has been shown that the discrete energy formulation for orthotropic curved plates as presented here provides a convenient and efficient matrix method for obtaining moments and deflections in curved plate structures with any boundary condition and loading.

Compared with the finite element method, the matrix manipulations are simpler since no integrations are involved. The number of unknown displacements to be evaluated are also less. Compared with the finite difference method, the resulting matrix is symmetrical. As a result, the complete formulation and solution can be efficiently and conveniently processed by a digital computer.

References

1. Coull, A. and Das, P. C.: Analysis of curved bridge decks. Proceedings, The Institution of Civil Engineers, London, May 1967, Vol. 37, pp. 75–85.
2. Yonezawa, H.: Moments and free vibrations in curved girder bridges. Proceedings of the American Society of Civil Engineers. Journal of the Engineering Mechanics Division, February 1962, Vol. 88, No. EM 1, Proceedings Paper 3052, pp. 1–21.
3. Heins, C. P., Jr., and Hails, R. L.: Behaviour of stiffened curved plate model. Proceedings of the American Society of Civil Engineers. Journal of the Structural Division, November 1969, Vol. 95, No. ST 11, Proceedings Paper 6876, pp. 2353–2370.
4. Bell, L. C. and Heins, C. P.: Analysis of curved girder bridges. Proceedings of the American Society of Civil Engineers. Journal of the Structural Division, August 1970, Vol. 96, No. ST 8, Proceedings Paper 7462, pp. 1657–1673.
5. Cheung, Y. K.: The analysis of cylindrical orthotropic curved bridge decks. Publications, International Association for Bridge and Structural Engineering, Vol. 29, Part 2, 1969, pp. 41–52.
6. Buragohain, D. N. and Ramesh, C. K.: A discrete analysis technique for folded plates with openings and overhangs. The Indian Concrete Journal, April 1971, Vol. 45, No. 4.
7. Buragohain, D. N. and Bhat, V. V.: Discrete analysis of curved plates in bending and plane stress. Proceedings of the symposium on "Recent developments in analytical, experimental and constructional techniques applied to engineering structures", held at Regional Engineering College, Warangal, India, on February 5–6, 1971.

Summary

The paper presents a method for analysing a curved bridge deck with arbitrary boundary conditions and loading and possessing cylindrical orthotropic material properties. Using classical thin plate theory in polar coordinates, extremum principles are utilised to derive element matrices for two classes of elements into which the structure is discretised: elements in bending and elements in twisting. Using matrix procedures, the entire formulation is automated on a digital computer. Comparison of results with available exact and approximate solutions shows the efficiency of the method.

Résumé

Le travail présente une méthode pour analyser la chaussée d'un pont courbe et orthotrope sous des conditions de limite et charges arbitraires. En utilisant la méthode classique sur les dalles minces dans les coordonnées polaires, on travaille avec des conditions extrêmes pour élaborer des matrices d'éléments pour les deux classes d'éléments en lesquelles la structure est divisée: éléments de flexion et éléments de torsion. En travaillant avec les procédures de matrices, la formulation entière est automatisée sur un computer digital. La comparaison des résultats avec des solutions exactes et approximatives disponibles montre l'efficacité de cette méthode.

Zusammenfassung

Die vorliegende Arbeit bietet eine Methode, um eine gekrümmte zylindrische orthotrope Brückenfahrbahn unter beliebigen Grenzbedingungen zu analysieren und zu belasten. Unter Anwendung der klassischen Theorie der dünnen Platten in Polarkoordinaten wird mit Extremalbedingungen gearbeitet, um diskretisierte Elementmatrizen zu gewinnen, in welchen die Struktur in Biegungs- und Drillelemente unterteilt ist. Bei Anwendung der Matrixverfahren wird die vollständige Formulierung automatisch von einem Digital-Computer ausgeführt. Der Vergleich der Resultate mit vorhandenen genauen und Näherungslösungen zeigt die Wirksamkeit dieser Methode.

Leere Seite
Blank page
Page vide